Biosensor Based on Self-Assembled Films of Graphene Oxide and Polyaniline Using a Field-Effect Device Platform

Danilo A. Oliveira,* Denise Molinnus, Stefan Beging, José R. Siqueira Jr,* and Michael J. Schöning*

A new functionalization method to modify capacitive electrolyte–insulator–semiconductor (EIS) structures with nanofilms is presented. Layers of polyallylamine hydrochloride (PAH) and graphene oxide (GO) with the compound polyaniline:poly(2-acrylamido-2-methyl-1-propanesulfonic acid) (PANI:PAAMPSA) are deposited onto a p-Si/SiO$_2$ chip using the layer-by-layer technique (LbL). Two different enzymes (urease and penicillinase) are separately immobilized on top of a five-bilayer stack of the PAH:GO/PANI:PAAMPSA-modified EIS chip, forming a biosensor for detection of urea and penicillin, respectively. Electrochemical characterization is performed by constant capacitance (ConCap) measurements, and the film morphology is characterized by atomic force microscopy (AFM) and scanning electron microscopy (SEM). An increase in the average sensitivity of the modified biosensors (EIS–nanofilm–enzyme) of around 15% is found in relation to sensors, only carrying the enzyme but without the nanofilm (EIS–enzyme). In this sense, the nanofilm acts as a stable bioreceptor onto the EIS chip improving the output signal in terms of sensitivity and stability.

D. A. Oliveira, Prof. J. R. Siqueira, Jr
Laboratory of Applied Nanomaterials and Nanostructures (LANNA)
Institute of Exact Sciences
Natural and Education
Federal University of Triângulo Mineiro (UFTM)
Uberaba 38064200, Brazil
E-mail: jose.siqueira@uftm.edu.br

D. A. Oliveira, Dr. D. Molinnus, S. Beging, Prof. M. J. Schöning
Institute of Nano- and Biotechnologies (INB)
Aachen University of Applied Sciences
Campus Jülich, 52428 Jülich, Germany
E-mail: schoening@fh-aachen.de

Prof. M. J. Schöning
Institute of Biological Information Processing (IBI-3)
Research Center Jülich
52425 Jülich, Germany

D. A. Oliveira
Fachhochschule Aachen
E-mail: daniloalves2902@hotmail.com

The ORCID identification number(s) for the author(s) of this article can be found under https://doi.org/10.1002/pssa.202000747.

1. Introduction

Long-term stable immobilization of the receptor layer (e.g., enzymes) is one of the most critical parts for the development of biosensors. Investigations show that the immobilization technique as well as conditions such as temperature, contaminants, and thickness of the enzyme membrane play a fundamental role in the subsequent performance of a biosensor and have a major effect on, for example, the sensitivity, drift, and long-term stability.[1–7] Typical immobilization techniques include drop coating, spin coating, and adsorptive binding or gel entrapment.[8–11] However, search for new approaches is fundamental in enhancement for devices resulting in improved sensor properties. Studies of field-effect devices (FEDs) for enzyme-based biosensors have shown that a better sensor performance can be achieved when the physical adsorption of the enzyme membrane is supported by an additional nanomaterial-based intermediate layer.[4,12–15] In this context, FEDs have become an interesting application for nanomaterials as enzyme carriers.[16]

In general, the working principle of a capacitive electrolyte–insulator–semiconductor (EIS) structure, which belongs to FEDs, is based on the fact that changes on the sensor surface can modulate its capacitance. This enables the detection of target molecules, presenting the advantages of being sensitive, small, of low weight, and resulting in low-cost devices.[17–20] Changes in pH, and as a consequence of hydronium and hydroxide ions, products of enzymatic reactions, can thus be monitored at the interface chip/electrolyte using such structures.[17–21]

The incorporation of enzymes and nanomaterials in the form of nanostructured films on FEDs has been shown to be an interesting strategy for enzyme immobilization to improve biosensors' performance.[18,19] In this sense, a simple and versatile method for modifying solid surfaces is the layer-by-layer (LbL) technique. It involves the principle of adsorption of molecules of opposite charges, being able to form multilayered films on a substrate using organic or inorganic molecules, polymers, natural proteins, or colloids.[22–24] The technique allows solutions using water as a solvent, depositing films on a wide variety of different substrates with molecular control and films on nanoscale. The application of nanomaterials, in addition, improves

the ability to catalyze reactions due to their high surface area.[5,18–20] One of the recent materials that can be incorporated is graphene oxide (GO), a graphene derivative where oxygen-containing functional groups, such as epoxy, hydroxyl, and carboxyl groups, cover the surface, which makes their use through the LbL technique relatively easy, as well as improving the interaction with target molecules.[25,26] For example, Liu et al. developed an amperometric biosensor using glucose oxidase and GO.[27] The authors observed that a distinct part of the sensor performance was due to the interaction of the oxygenated groups, especially the oxide carboxylics, with the amino groups of the glucose oxidase. In another approach, Xu et al. developed an aggregation-induced emission (AIE) biosensor to detect bovine serum albumin (BSA).[28] In this study, the presence of GO was fundamental, solving the normal drawback of low selectivity of AIE sensors and resulting in increased sensitivity. Recently, Vajedi and Dehghani reported the combination of GO with layered double hydroxides (LDHs) and cobalt ferrite ($CoFe_2O_4$) on a fluorine tin oxide (PTO) substrate as an electrochemical DNA (deoxyribonucleic acid) biosensor. They observed reproducibility, stability, and selectivity, as well as sensing in real samples such as human blood plasma, serum, and urine with good recovery.[29] The developed sensor had active sites allowing interaction with the target molecule. In addition, being capable of immobilization of DNA, the sensor facilitates the transfer of electrons on the electrode surface.

Polyaniline (PANI), the second material of this study, has been used by researchers due to its easy availability, conductivity, stability, and operation at room temperature.[30,31] Its use in energy storage systems is well known due to the increase in capacitance generated through its pseudocapacitive effect.[32,33] For application in field-effect sensors, this material still has potential to be more explored, especially in combination with nanomaterials. For instance, Dhaoui et al. reported the detection of nitrite[34] by modifying a Si/SiO_2 structure with PANI and sulfamic acid (abbreviated PANI-SFA), achieving a significant increase in sensitivity.

In this study, a capacitive field-effect sensor has been developed with a nanomaterial-assisted surface supported by a polyelectrolyte polyallylamine hydrochloride (PAH):GO/PANI:PAAMPSA (poly(2-acrylamido-2-methyl-1-propanesulfonic acid)) layer stack with the enzymes urease and penicillinase, respectively, chosen as model enzymes. The two model enzymes have been selected with regard to possible future biomedical applications: A high concentration of urea, a metabolite of the organism, is an indication of renal failure, dehydration, urinary tract obstruction, burns, shocks, and gastrointestinal bleeding.[35,36] Penicillin G, as an antibiotic substance, can sometimes cause allergic shocks in patients and is applied in veterinary medicine.[37] Electrochemical constant capacitance (ConCap) analysis associated with morphological images by scanning electron microscopy (SEM) and atomic force microscopy (AFM) have demonstrated that the presence of the nanofilm plays an important role in stabilizing the enzyme immobilization over the EIS chip, leading to urea and penicillin biosensors with 15% higher sensitivity and improved output signal in terms of signal response and long-term stability in comparison with a nanofilm-free biosensor.

2. Experimental Section

2.1. Materials and Solutions

GO functionalized with carboxylic acid and PAH (average 54 Mw = 58 000) were acquired from Sigma-Aldrich (Germany). Titrisol buffer, tris(hydroxymethyl)amonomethane, potassium dihydrogen phosphate, citric acid, disodium tetraborate, potassium chloride, urease (*Canavalia ensiformis* made of Jack beans, 50 000−100 000 units/g solid), urea, penicillinase (*Bacillus cereus*, specific activity: 1670 units/mg protein), and penicillin G (benzyl penicillin) were also purchased from Sigma-Aldrich, as well as the buffer components (monosodium phosphate and disodium phosphate) for the preparation of phosphate buffer solution (PBS).

For the PANI synthesis, dimethylacetamide (DMAc), hydrochloric acid, aniline, (3-aminopropyl)triethoxysilane (APTES), propylene carbonate, lithium perchlorate, and ammonium peroxydisulfate were purchased from Sigma-Aldrich (United States). PAAMPSA (10.36 wt% in water, $M_w \approx 800\,kg\,mol^{-1}$) was purchased from Scientific Polymer Products (United States).

2.2. Polymix Buffer Preparation

Tris(hydroxymethyl)aminomethane (3.03 g), 3.40 g of potassium dihydrogen phosphate, 5.25 g of citric acid, 5.03 g of disodium tetraborate, and 1.86 g of potassium chloride were dissolved in 1 L of distilled water. The resulting polymix buffer with a concentration of 25×10^{-3} M was diluted to 0.25 and 100×10^{-3} M of potassium chloride was added.

2.3. PANI-PAAMPSA Synthesis

Synthesis of PANI:PAAMPSA was performed according to previous reports.[38,39] A total of 5.8 g of PAAMPSA (0.028 M) was dissolved in 375 mL of deionized water, and 2.6 g of aniline was added to the PAAMPSA solution and stirred for 1 h. Ammonium peroxydisulfate (5.8 g) was also dissolved in 25 mL of deionized water separately. This last solution was added dropwise to the first one, and polymerization was conducted at 5 °C for 24 h. Then, acetone was added to precipitate the PANI:PAAMPSA, which was filtered and washed with acetone to remove the unreacted monomer and oligomer. The isolated emeraldine salt PANI:PAAMPSA colloid (green color) was dried under vacuum at room temperature overnight.

2.4. Fabrication of EIS Structures

The fabrication process of the EIS sensors followed the procedure mentioned before with SiO_2 as pH-sensitive transducer material fabricated my means of thin-film technology.[18] The EIS chips were fabricated with an $Al/p-Si/SiO_2$ layer sequence. For this, a p-doped Si substrate (356–406 μm thick) with a specific resistance of 1–5 Ω cm was used. The SiO_2 layer was produced by thermal oxidation of the Si under O_2 atmosphere at 1050 °C for 30 min, resulting in a thickness of ≈30 nm. A 300 nm thick Al contact layer was deposited on the rear side of the p-Si by electron-beam evaporation, which was annealed

afterward. The wafer was cut with a diamond saw into single chips of $1.0\,cm^2$ sizes. The chips were cleaned in acetone (5 min), after that in isopropanol (5 min), and finally in deionized water (10 min). Before modification of the surface of the EIS sensors, they were placed in a homemade acrylic measuring cell and sealed by an O-ring. The active area of the chip exposed to the solution was $0.5\,cm^2$.

2.5. LbL Film Preparation and Enzyme Immobilization

The PAH:GO dispersion at pH 4 was obtained by solving 10 mg of PAH and 5 mg of GO in 10 mL of deionized water, which was then ultrasonicated for 2 h. The solution containing PANI:PAAMPSA was made following the procedure described in the literature[40]: 5 mg of PANI:PAAMPSA was dispersed in 10 mL of deionized water, sonicated, and the pH was adjusted to pH 2.5 using diluted HCl. For modification of the EIS sensors via the LbL technique, the chips were immersed in the PAH:GO solution for 10 min, washed three times with distilled water, dried with nitrogen, and added to the PANI:PAAMPSA solution for 10 min, also washed three times with distilled water, and dried with nitrogen, forming a bilayer. Based on previous reports from the current study's group, considering the use of amine-functionalized polyelectrolytes (PAH and PANI:PAAMPSA) and a carbon-based nanomaterial functionalized with carboxylic acid, the number of bilayers to fabricate the PAH:GO/PANI:PAAMPSA was set to five.[14,18–20,41,42]

The enzyme cocktail with urease was prepared by dissolving 30 mg of enzyme powder in 15 mL of 0.25×10^{-3} M polymix buffer solution, pH 7. Urea solutions were prepared at different concentrations ranging from 0.1 to 100×10^{-3} M in a 0.25×10^{-3} M polymix buffer solution, pH 8, containing 100×10^{-3} M of KCl. The penicillinase solution was prepared by dissolving 1.8 mg of the enzyme powder in 1 mL of 0.2 M triethanolamine (TEA) buffer, pH 8. The penicillin solutions of different concentrations ranging from 0.1 to 50×10^{-3} M were prepared by dissolving penicillin G in a 0.25×10^{-3} M polymix buffer, pH 8, containing 100×10^{-3} M of KCl. Both enzyme solutions (80 µL each) were physically adsorbed onto the PAH:GO/PANI:PAAMPSA layer stack, left overnight to complete the immobilization procedure, and nonspecific bound enzyme

was removed by washing steps before starting the measurement. The resulting bioreceptor nanofilm and the scheme of the measurement setup including the sensor chip are shown in **Figure 1**.

2.6. Physical and Electrochemical Characterization

To study the influence of the additional nanofilm on the sensor performance, nanofilm-modified EIS sensors (by LbL technique) including the particular enzyme were compared with bare EIS sensors only carrying the enzyme (urea or penicillinase) without the nanofilm. In this case, 80 µL of the respective enzyme solution was drop coated onto the sensor surface and immobilized overnight.

The surface of the functionalized EIS sensors was analyzed with an atomic force microscope BioMat Workstation (JPK Instruments, Germany) and a field-emission scanning electron microscope (Jeol JSM – 7800F, Germany). Tapping mode liquid-cell AFM images were taken using Si cantilevers with silicon nitride tips. The scanned area was $2\,\mu m^2$. The root-mean-square (rms) roughness of the multilayer PAH:GO/PANI:PAAMPSA were estimated by data analysis using the software Gwyddion SPM.

The differently prepared biosensors were characterized by means of ConCap mode measurement at a frequency of 70 Hz using an impedance analyzer (Zahner Elektrik, Germany). An alternating current (AC) voltage with an amplitude of 20 mV was used for all measurements. The working capacitance for the ConCap mode was defined by carrying out $C–V$ (capacitance–voltage) measurements in a direct current (DC) voltage range between -2 and 2 V with steps of 100 mV. The capacitance in the linear range of the depletion region ($\approx$60% of the maximum capacitance) was chosen (data not shown).[4,12,13] In the ConCap mode, the capacitance of the EIS sensor was kept constant using a feedback-control circuit that allows the direct monitoring of potential changes at the sensor surface. A conventional liquid-junction Ag/AgCl electrode (Metrohm, Germany) was used as a reference electrode. The measurements were performed in a dark Faraday cage at room temperature with $n = 3$ sensors for statistical evaluation. For pH and urea detection, a conditioning time of 5 min was used; for penicillin, it was 6 min.
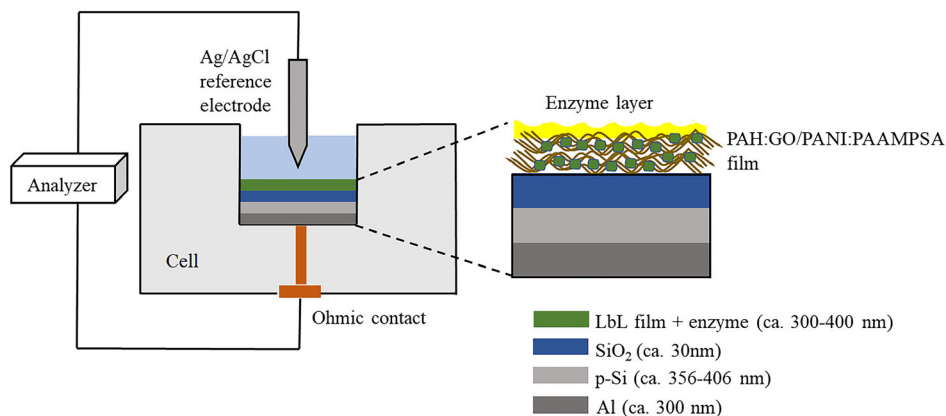
Figure 1. Schematic representation of the measurement setup with the EIS sensor modified by the PAH:GO/PANI:PAAMPSA LbL film with the enzyme urease and penicillinase, respectively.

3. Results and Discussion

3.1. Surface Morphology

Five bilayers of an LbL stack of PAH:GO/PANI:PANI:PAAMPSA were prepared, based on former experiments with nanofilms, that turned out to provide their best performance in terms of sensitivity.[14,18,41] **Figure 2** shows SEM pictures of the surface morphology of a p-Si/SiO$_2$ EIS chip with enzyme penicillinase (left) and a modified EIS sensor with a five-bilayer PAH:GO/PANI: PAAMPSA/penicillinase LbL nanofilm (right). In comparison to the unmodified chip, the interaction between PANI and the graphene sheet is clearly demonstrated in the five-bilayer arrangement: There is an increase in the surface area of the nanofilms (see right SEM image), which provides a randomly higher surface coverage over the entire chip surface. Based on previous studies of our group, the structure of the nanofilm may act as a membrane in which a better enzyme adhesion can be expected.[14,18,41] At the same time, on the other hand, one should mention that too many bilayers might probably isolate the oxide surface, also hindering ions from diffusing to the sensor surface, and decrease the sensitivity.[14,18,41]

In **Figure 3**, a sensor with the nanofilm and urease (a) and a bare EIS sensor modified by the enzyme urease (b) are exemplarily shown by AFM images in a scan area of ≈2 µm^2. The sensor modified with the nanofilm and urease exhibits a typical topography containing stacked GO sheets randomly oriented over the chip surface, which can be visualized as indicated by the blue arrows in Figure 3a (left). The irregular surface (nonflat) leads to a high surface area with an rms roughness of ≈16.0–20.0 nm, in which the aggregates in lighter regions may indicate the intense presence of the enzyme immobilized over the film surface, as displayed in the 3D image (right). In contrast, the bare EIS sensor (Figure 3b) shows a regular topographic profile with a lower rms roughness of ≈6.0–9.0 nm, as expected. Also different, the presence of aggregates on the surface (lighter regions) is not intense, indicating that the presence of the nanofilm promotes the incorporation of a higher amount of enzyme and better distribution over the chip surface. These changes

in the morphological properties for films with a rougher active surface area is desirable as they can permit the formation of sensor units (bioreceptor) that can promote an improvement in properties and better performance, such as higher sensitivity and stable output signals.[14,18–20,41] It is worth mentioning that similar features in the topographic profile were observed for EIS sensors modified with nanofilm and penicillinase (data not shown).

3.2. pH Sensitivity of the EIS Structure Functionalized with LbL Film

The influence of the PAH:GO/PANI:PAAMPSA nanofilm containing five bilayers on the pH sensitivity of the capacitive EIS sensor was proven. Therefore, a bare EIS sensor and a sensor modified with the nanofilm (both without enzymes) were characterized in Titrisol buffer at different pH values ranging from pH 5 to 9. Exemplary ConCap recordings are displayed in **Figure 4**. The measurements started at pH 5 and continued to pH 9 in increments of 1, and again backward to pH 5. Each pH value was recorded for 5 min. The black curve corresponds to the measurement of the blank EIS sensor and the red one to the sensor modified with the nanofilm. In both cases, the signals were stable for all pH values and showed distinct steps for varying concentrations. The hysteresis at pH 7 amounted to be ≈4 mV. There was no different behavior in terms of average pH sensitivity. As shown in Figure 4b, for the bare EIS sensor a mean sensitivity of 54.6 ± 2.7 mV pH^{-1} and for the EIS sensor modified by the nanofilm, a mean sensitivity of 53.9 ± 2.2 mV pH^{-1} were achieved. These values are comparable to literature data[7] and indicate that the nanofilm did not isolate the surface of the EIS chip, allowing the H$^+$ ions to have access to the SiO$_2$ hydroxyl surface groups. Overall, these results corroborate those of the AFM and SEM images in Figure 2 and 3, respectively, where it was observed that although the nanofilm is distributed evenly over the chip surface, there are still open areas exposed for interaction of electrolyte ions with the sensor surface.
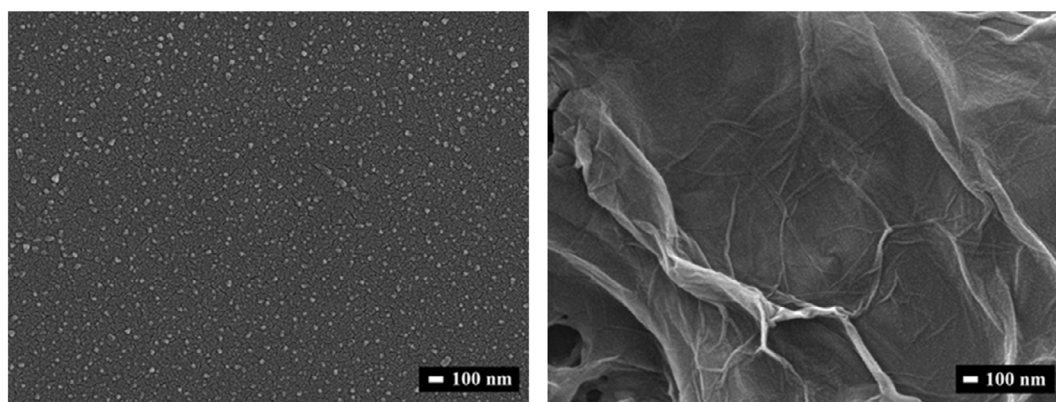
Figure 2. SEM images of an EIS field-effect sensor with enzyme penicillinase (left) and an EIS sensor with a five-bilayer stack of PAH:GO/PANI: PAAMPSA/penicillinase (right) at 33 000× magnification; energy of e-beam: 5 kV.
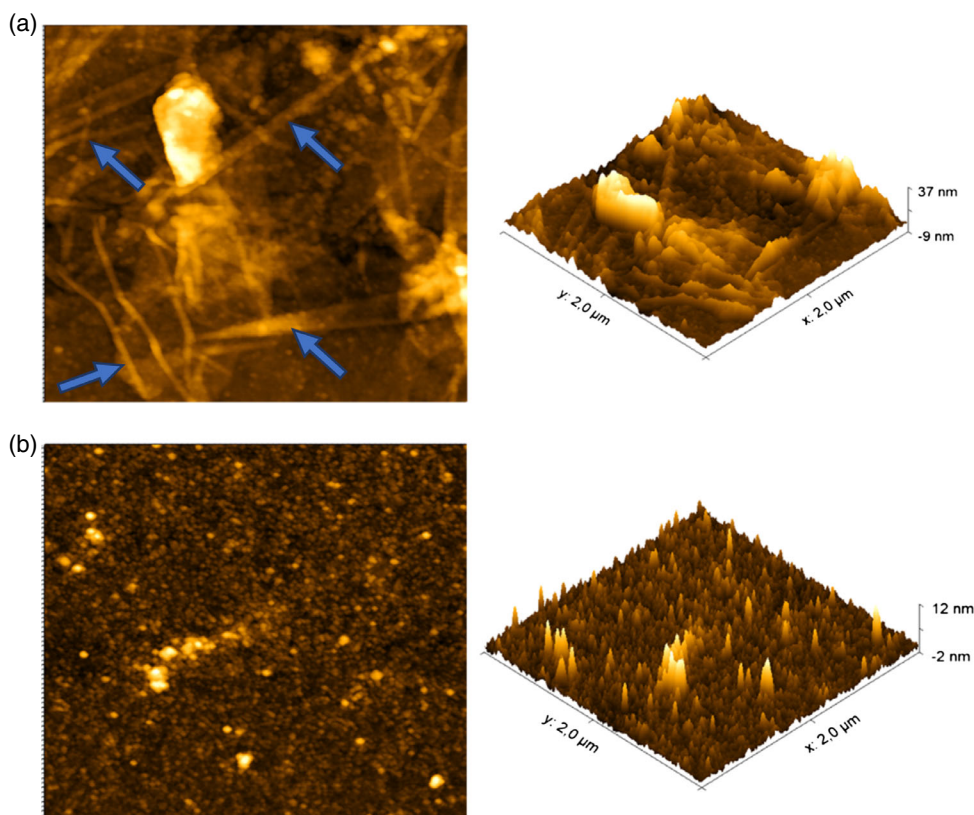
Figure 3. AFM images for the a) enzyme urease immobilized on top of a five-bilayer PAH:GO/PANI:PAAMPSA LbL film and for the b) bare EIS sensor with the immobilized enzyme urease and their respective 3D images. Blue arrows indicate GO sheets, randomly oriented over the film surface.

3.3. Urea Sensitivity of the EIS Structure Functionalized with LbL Film

Among the ways of detecting urea, immobilization by adsorption of the enzyme urease on the field-effect sensor surface presents the disadvantage of having a short lifetime, often making the reuse of such sensors limited.[43–45] To circumvent this drawback, films between the EIS sensor surface and the physically adsorbed enzyme can improve the immobilization stability and sensitivity.[43] To study this effect, a nanofilm of LbL PAH:GO/PANI:PAAMPSA with urease was chosen. Urease acts by hydrolyzing one urea molecule to one carbon dioxide and two ammonia molecules, which hydrolyze into ammonium and hydroxide ions. Thus, after the reaction, an increase in pH directly at the sensor surface is expected and in this way, this pH change can be detected by the sensor.[21] In **Figure 5**a, exemplarily ConCap curves for urea detection involving the EIS sensor modified by the nanofilm of LbL-deposited PAH:GO/PANI:PAAMPSA with enzyme urease and the bare EIS sensor with enzyme urease in a linear concentration range between 0.1 and 100×10^{-3} M urea are presented with their respective sensitivities (see Figure 5b). For statistical evaluation, three sensors each ($n = 3$) were prepared (EIS sensor modified by the nanofilm and enzyme; bare EIS sensor modified by the enzyme). The measurements were started by measuring in polymix buffer solution (pH 8) for 5 min, followed by different urea concentrations

starting with 0.1×10^{-3} M urea. The concentrations were increased stepwise until 100×10^{-3} M urea, decreased again to the lowest concentration of 0.1×10^{-3} M urea, ending up with the polymix buffer solution. As described by the theory, the sensor signal increased with increasing urea concentration due to the increase of the pH value.[17]

For the nanofilm-modified EIS sensor, an average urea sensitivity of 41 ± 0.1 mV dec^{-1} was achieved, whereas the EIS sensor without nanofilm exhibited an average value of 35 ± 1.2 mV dec^{-1}. The data have been evaluated from $n = 3$ sensors each, taken into account the respective calibration curves in Figure 5b. The ≈15% higher sensitivity of the nanofilm-modified sensor chip in relation to the nonmodified sensor chip can be probably explained by the presence of the nanofilm, which provided a higher enzyme loading onto the sensor surface due to its increased morphological architecture. At concentrations higher than examined (data not shown), both sensors show a saturation behavior: The amount of urea on the sensor surface requires more time to be converted by the enzyme and at the same time, having high urea concentrations results in our experiment in a strong pH increase of about $\Delta pH \approx 2$, decreasing the activity of the enzyme dramatically.[14]
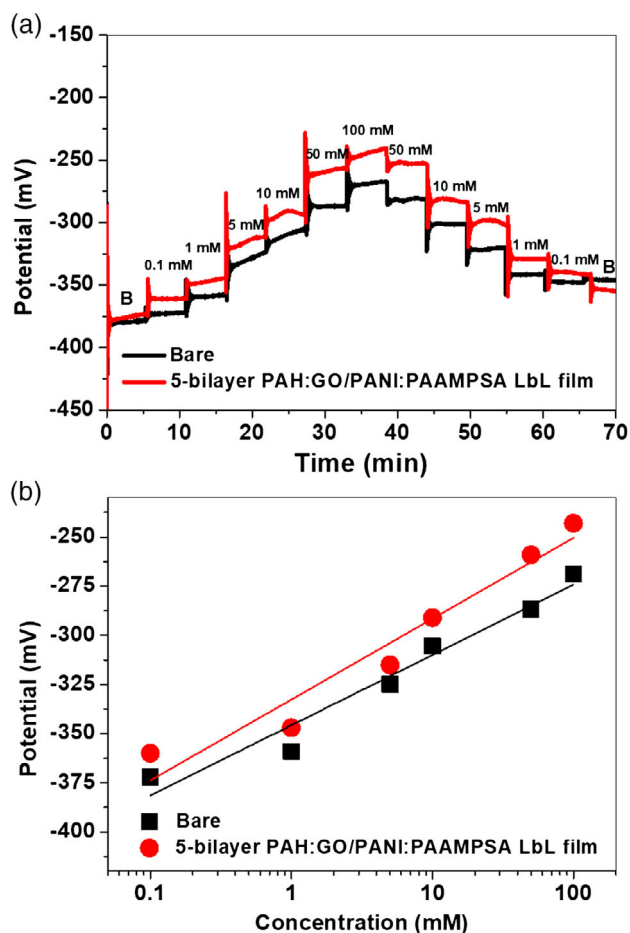
The stability of both urea biosensors was also investigated (data not shown). In case of the LbL-modified biosensor, the average urea sensitivity dropped from ≈41 to ≈30 mV dec^{-1} within the first three days, whereas for the nanofilm-free urea biosensor,
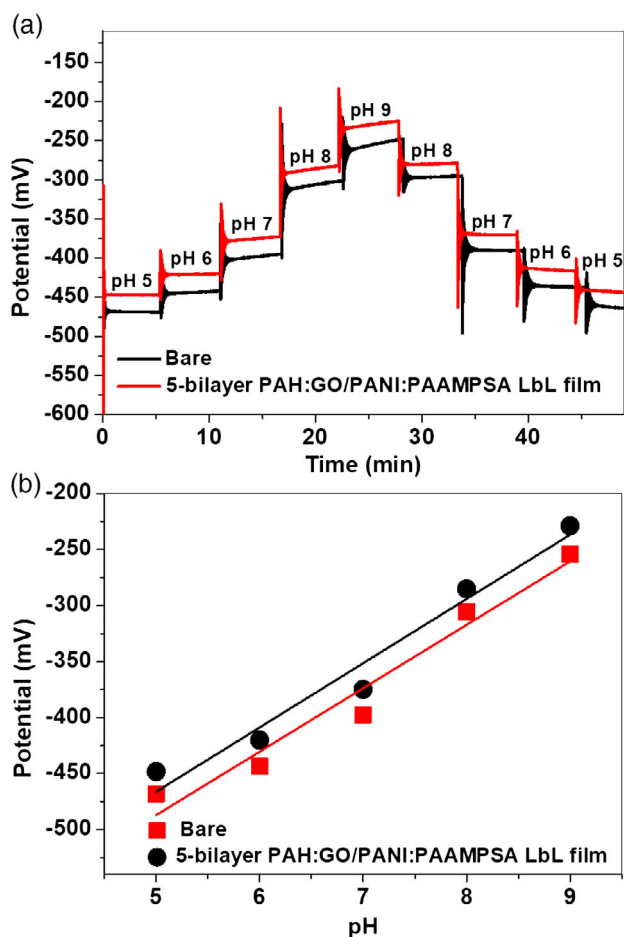
Figure 4. a) ConCap measurement of different pH values (pH 5–9) of a bare EIS sensor (black line) and an EIS sensor modified by a five-bilayer nanofilm of PAH:GO/PANI:PAAMPSA (red line); b) corresponding calibration curves for both sensor variants.

Figure 5. a) ConCap measurement of different urea concentrations ($0.1–100 \times 10^{-3}$ M) of a bare EIS sensor with immobilized urease (black line) and an EIS sensor modified by a five-bilayer nanofilm of PAH:GO/PANI:PAAMPSA with immobilized urease (red line); b) corresponding calibration curves for both sensor types. B: buffer.

the signal decreased from ≈35 to ≈18 mV dec^{-1}. A possible explanation for this behavior might be associated with a larger amount of enzyme being distributed and better accommodated over the high surface area of the film and interactions between the outermost polymeric layer and the enzyme, causing better incorporation (adhesion) onto the film. The obtained urea sensitivities for the LbL-modified biosensor are in good agreement (and even slightly higher) with results reported by, for example, Siqueira Jr. et al.,[14] who developed an LbL nanofilm consisting of a polyamidoamine (PAMAM) dendrimer and carbon nanotubes (CNTs) on an EIS sensor platform, with sensitivities of around 33 mV dec^{-1}, and Wu et al.,[46] who also investigated an EIS platform with Sm_2O_3 as the pH-transducing layer with immobilized urease. The authors observed a sensitivity of 2.5 mV mM^{-1} in the urea concentration range of $5–40 \times 10^{-3}$ M. Similar results were discussed by Wu et al. with a urea sensitivity of 9.59 mV mM^{-1} in the concentration range from 1 to 16×10^{-3} M.[47]

The ConCap cycle in Figure 5a underlines more pronounced steps in case of the nanofilm-modified urea biosensor, making it
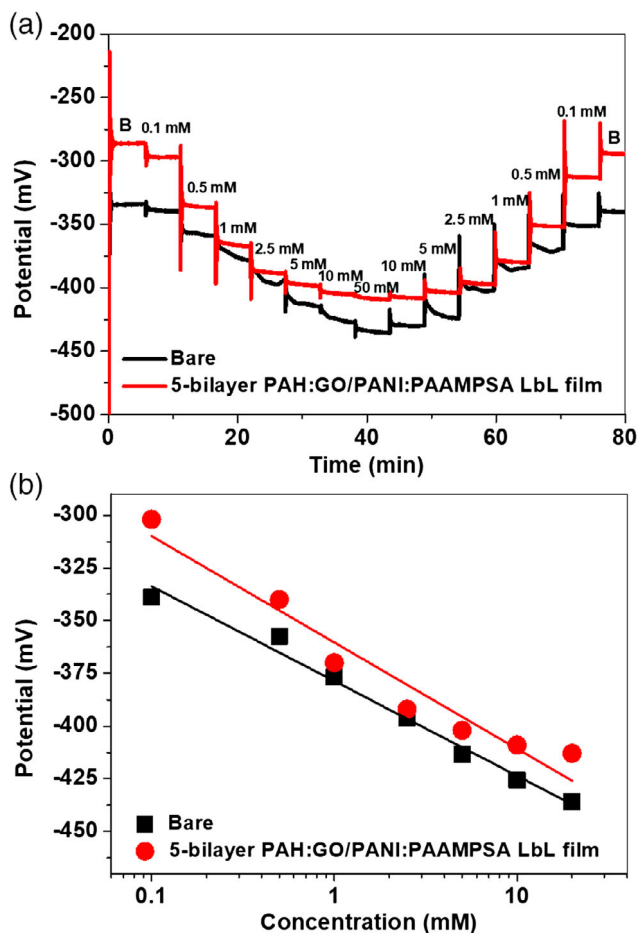
an appropriate possible candidate for further monitoring of urea in human samples, such as blood and urine. The lowest urea concentration examined in this experiment of 0.1×10^{-3} M indicates that the sensor can be principally used to detect urea in human serum (estimated to be in the range of $1.7–8.3 \times 10^{-3}$ M).[48]

3.4. Penicillin Sensitivity of the EIS Structure Functionalized with LbL Film

As a second model enzyme, penicillinase was chosen to modify a bare EIS sensor and a sensor with the already implemented nanofilm. Upon the addition of penicillin, the immobilized penicillinase catalyzes the hydrolysis of penicillin to penicilloic acid, resulting in the production of H$^+$ ions.[49] Thus, the potential during ConCap mode measurement is expected to decrease as the concentration of penicillin in the solution is increased. **Figure 6** shows two ConCap graphs obtained from the bare EIS sensor modified with penicillinase (black line) and the EIS sensor modified by the nanofilm and penicillinase (red line). Penicillin concentrations between 0.1 and 50×10^{-3} M were

Figure 6. a) ConCap measurement of different penicillin concentrations (0.1–50×10^{-3} M) of a bare EIS sensor with immobilized penicillinase (black line) and an EIS sensor modified by a five-bilayer nanofilm of PAH:GO/PANI:PAAMPSA with immobilized penicillinase (red line); b) corresponding calibration curves for both sensor types. B: buffer.

penicillin sensitivity exists for the nanofilm-modified sensor chip, whose improved sensor performance can be explained by the modified surface architecture. Both sensors have a pretty high long-term stability; even after 30 days, no loss in sensitivity was found, which was still ≈ 43 mV dec^{-1} for the bare EIS sensor and 50 mV dec^{-1} for the modified EIS sensor.

To interpret the achieved results in terms of lower detection limit and linear measurement range with literature data, Koch et al. used tobacco mosaic virus (TMV) nanorods together with penicillinase for an acidimetric penicillin detection performed with bromocresol purple as pH indicator and spectrophotometry, yielding a lower detection limit of 100×10^{-6} M.[37] Healey and Walt described an optical penicillin biosensor also based on the enzyme penicillinase, where the sensor is made by selective photodeposition of analyte-sensitive polymer matrices on optical imaging fibers. This sensor detects penicillin in the concentration range from 0.25 to 10.0×10^{-3} M.[50] Lee et al. utilized a charge-transfer technique for constructing a penicillin biosensor by immobilizing the enzyme penicillinase onto Si_3N_4 as pH transducer material.[51] They detected variations in the H$^+$-ion concentration resulting from the catalyzed hydrolysis of penicillin by the enzymatic reaction, delivering a penicillin sensitivity of 47.8 mV mM^{-1} in the linear concentration range from 0 to 25×10^{-3} M, and having a detection limit of about 10×10^{-6} M.

Beging et al.[52] investigated a nanospotting technique for deposition of penicillinase onto a capacitive field-effect EIS structure of Al/p-Si/SiO$_2$/Ta$_2$O$_5$. Penicillin sensitivity calculated from the respective C–V curves was similar, with 46.7 mV dec^{-1} in the concentration range from 0.5 to 10×10^{-3} M. Another capacitive field-effect EIS structure was reported by Poghossian et al.[16] The study involved the surface modification of the Al/p-Si/SiO$_2$/Ta$_2$O$_5$ field-effect structure by TMV nanotubes as penicillinase nanocarrier for enhanced biosensing. A further example is discussed with an LbL film, consisting of layers of polyaminoamide (PAMAM) and single-walled carbon nanotubes (SWNTs) used in FEDs and modified by a layer of penicillinase atop.[41] In other approach, Ibupoto et al. fabricated a penicillinase biosensor based on zinc oxide (ZnO) nanorods on a gold-coated glass substrate using a low-temperature aqueous chemical growth method. The enzyme was immobilized with ZnO nanorods and ANB-NOS (N-5-azido-2-nitrobenzoyloxysuccinimide) as cross-linker. Also, here, a good linearity over a wide concentration range from 100×10^{-6} M to 100×10^{-3} M was obtained.[53]

Despite the fact that these penicillin sensors for some examples possess even higher penicillin sensitivity, it should be mentioned that PANI in FED structures represents a new topic: Its dual use—as material for energy storage systems and simultaneous application to define a "soft architecture" for embedding biomolecules with regard to immobilization—offers to be a promising candidate for further optimization steps in the field of biosensing.

4. Conclusion

A capacitive field-effect EIS sensor was prepared with nanomaterial-modified films containing reduced GO and PANI on a SiO$_2$ surface. The properties of this new type of sensor surface were compared with a bare EIS sensor by performing

tested. Each concentration was recorded for 6 min. In the beginning, the respective sensor was measured in buffer solution (polymix buffer, pH 8), followed by the lowest penicillin concentration of 0.1×10^{-3} M and increasing up to 50×10^{-3} M. After measuring 50×10^{-3} M penicillin, the concentration was again decreased to 0.1×10^{-3} M. Before finishing the experiment, the sensor signal was recorded by measuring only in the buffer solution. As for the urea biosensor, both sensor types show a similar sensor behavior. Remarkably, the signal steps for the different penicillin concentrations are even more pronounced in case of the nanofilm-modified field-effect biosensor. For both sensor variants, the sensor signal is decreasing with increasing penicillin concentration and vice versa. The calibration plots in Figure 6b show an average penicillin sensitivity of 43.2 ± 4.3 mV dec^{-1} for the bare EIS sensor with immobilized penicillinase and 50.7 ± 3.9 mV dec^{-1} of the modified EIS sensor with the nanofilm and immobilized penicillinase, in the linear concentration range between 0.1 and 50×10^{-3} M penicillin. The measurements have been performed for $n = 3$ sensors for each variant. Also in this experiment, an $\approx 15\%$ higher average

ConCap measurements at different pH values. Results showed that the additional nanofilm did not negatively influence the intrinsic pH sensitivity of the Al/p-Si/SiO$_2$ field-effect sensor.

To prove the benefit of the nanofilm in terms of bioreceptor coupling, two enzymes were immobilized on top of the new layer stack, that is, penicillinase and urease, both selected as model enzymes. In AFM and SEM characterizations, it was possible to observe an increase in the surface area due to the nanofilm, which is crucial to improve enzyme immobilization and chip/analyte interaction. In ConCap analysis, the modified sensor with nanofilm and the respective enzyme showed improved sensor performance in terms of sensitivity, stability, and signal drift over the sensor modified only by the enzyme and without a nanofilm. Based on these fundamental "proof of concept" experiments, we plan to extend this study to further different enzymes and to systematically investigate the layer numbers of the LbL stack of PAH:GO/PANI:PAAMPSA when coupling the enzymes.

Conflict of Interest

The authors declare no conflict of interest.

Data Availability Statement

Research data are not shared.

[1] N. J. Ronkainen, H. B. Halsall, *Chem. Soc. Rev.* **2010**, *39*, 1747.

[2] E. Katz, I. Willner, *Electroanalysis* **2003**, *15*, 913.

[3] B. Krajewska, *Enzyme Microb. Technol.* **2004**, *35*, 126.

[4] D. Molinnus, L. Muschallik, L. O. Gonzalez, J. Bongaerts, T. Wagner, T. Selmer, P. Siegert, M. Keusgen, M. J. Schöning, *Biosens. Bioelectron.* **2018**, *115*, 1.

[5] G. Dhawan, G. Sumana, B. D. Malhotra, *Biochem. Eng. J.* **2009**, *44*, 42.

[6] A. Poghossian, M. Thust, P. Schroth, A. Steffen, H. Lüth, M. J. Schöning, *Sens. Mater.* **2004**, *13*, 207.

[7] A. Poghossian, M. J. Schöning, *Encyclopedia of Sensors* (Eds: C. A. Grimes, E. C. Dickey, M. V. Pishko), Vol. 9, American Scientific Publishers, Stevenson Ranch (USA) **2006**, p. 463.

[8] W. Ma, Q. Jiang, P. Yu, L. Yang, L. Mao, *Anal. Chem.* **2013**, *85*, 7550.

[9] Y. Xin, X. Fu-bing, L. Hong-wei, W. Feng, C. Di-zhao, W. Zhao-yang, *Electrochim. Acta* **2013**, *109*, 750.

[10] J. Liu, M. Agarwal, K. Varahramyan, *Sens. Actuators, B* **2008**, *135*, 195.

[11] A. Sassolas, L. J. Blum, B. D. Leca-bouvier, *Biotechnol. Adv.* **2012**, *30*, 489.

[12] D. Molinnus, S. Beging, C. Lowis, M. J. Schöning, *Sensors* **2020**, *20*, 4924.

[13] M. J. Schöning, N. Näther, V. Auger, A. Poghossian, M. Koudelka-Hep, *Sens. Actuators, B* **2005**, *108*, 986.

[14] J. R. Siqueira Jr., D. Molinnus, S. Beging, M. J. Schöning, *Anal. Chem.* **2014**, *86*, 5370.

[15] D. Sarkar, W. Liu, X. Xie, A. C. Anselmo, S. Mitragotri, K. Baneriee, *ACS Nano* **2014**, *8*, 3992.

[16] A. Poghossian, M. Jablonski, C. Joch, T. S. Bronder, D. Rolka, C. Wege, M. J. Schöning, *Biosens. Bioelectron.* **2018**, *110*, 168.

[17] A. Poghossian, M. J. Schöning, *Sensors* **2020**, *20*, 5639.

[18] P. V. Morais, A. C. A. Silva, N. O. Dantas, M. J. Schöning, J. R. Siqueira Jr, *Phys. Status Solidi A* **2019**, *216*, 1900044.

[19] P. V. Morais, V. F. Gomes Jr., A. C. A. Silva, N. O. Dantas, M. J. Schöning, J. R. Siqueira Jr., *J. Mater. Sci.* **2017**, *52*, 12314.

[20] J. R. Siqueira Jr., M. H. Abouzar, A. Poghossian, V. Zucolotto, O. N. Oliveira Jr., M. J. Schöning, *Biosens. Bioelectron.* **2009**, *25*, 497.

[21] P. Kumar, S. Maikap, K. Singh, S. Chatteriee, Y. Y. Chen, H. M. Cheng, R. Mahapatra, J. T. Qiu, J. R. Yang, *J. Electrochem. Soc.* **2016**, *163*, B580.

[22] G. Decher, M. Eckle, J. Schmitt, B. Struth, *Curr. Opin. Colloid Interface Sci.* **1998**, *3*, 32.

[23] K. Ariga, Y. Yamauchi, G. Rydzed, Q. Ji, Y. Yonamine, K. C. W. Wu, J. P. Hill, *Chem. Lett.* **2014**, *43*, 36.

[24] Y. Lvov, K. Ariga, I. Ichinose, T. Kunitake, *J. Am. Chem. Soc.* **1995**, *117*, 6117.

[25] K. Toda, R. Furue, S. Hayami, *Anal. Chim. Acta* **2015**, *878*, 43.

[26] D. Zhang, J. Tong, B. Xia, Q. Xue, *Sens. Actuators, B* **2014**, *203*, 263.

[27] Y. Liu, D. Yu, C. Zeng, Z. Miao, L. Dai, *Langmuir* **2010**, *26*, 6158.

[28] X. Xu, J. Huang, J. Li, J. Yan, J. Qin, Z. Li, *Chem. Commun.* **2011**, *47*, 12385.

[29] F. S. Vajedi, H. Dehghani, *Talanta* **2020**, *208*, 120444.

[30] T. Sen, S. Mishra, N. G. Shimpi, *RSC Adv.* **2016**, *6*, 42196.

[31] I. G. Casella, T. R. I. Cataldi, A. Guerrieri, E. Desimoni, *Anal. Chim. Acta* **1996**, *335*, 217.

[32] A. Eftekhari, L. Li, Y. Yang, *J. Power Sources* **2017**, *347*, 86.

[33] H. Zhou, H. Chen, S. Luo, G. Lu, W. Wei, Y. Kuang, *J. Solid State Electron.* **2005**, *9*, 574.

[34] W. Dhaoui, M. Bouzitoun, H. Zarrouk, H. B. Ouada, A. Pron, *Synth. Met.* **2008**, *158*, 722.

[35] J. W. Schrock, M. Glasenapp, K. Drogell, *Clin. Neurol. Neurosurg.* **2012**, *114*, 881.

[36] A. Barik, S. Upadhyaya, I. U. Muzaddadi, N. S. Sarma, in *IEEE Sensors*, IEEE **2018**, pp. 1–4.

[37] C. Koch, A. Poghossian, M. J. Schöning, C. Wege, *Nanotheranostics* **2018**, *2*, 184.

[38] J. E. Yoo, J. L. Cross, T. L. Bucholz, K. S. Lee, M. P. Espe, Y. Loo, *J. Mater. Chem.* **2007**, *17*, 1268.

[39] J. Jeon, Y. Ma, J. F. Mike, L. Shao, P. B. Balbuena, J. L. Lutkenhaus, *Phys. Chem. Chem. Phys.* **2013**, *15*, 9654.

[40] J. W. Jeon, J. O'Neal, L. Shao, J. L. Lutkenhaus, *ACS Appl. Mater. Interfaces* **2013**, *5*, 10127.

[41] J. R. Siqueira Jr., M. H. Abouzar, M. Bäcker, V. Zucolotto, A. Poghossian, O. N. Oliveira, M. J. Schöning Jr., *Phys. Status Solidi A* **2009**, *206*, 462.

[42] M. A. M. Sousa, J. R. Siqueira Jr., A. Vercik, M. J. Schöning, O. N. Oliveira Jr., *IEEE Sens. J.* **2017**, *17*, 1735.

[43] K. Kim, J. Lee, B. M. Moon, Y. B. Seo, C. H. Park, M. Park, G. Y. Sung, *Sensors* **2018**, *18*, 2607.

[44] K. Rafiq, H. D. Mai, J. K. Kim, J. M. Woo, B. M. Moon, C. H. Park, H. Yoo, *Sens. Actuators, B* **2017**, *251*, 472.

[45] A. Sassolas, L. J. Blum, B. D. Leca-bouvier, *Biotechnol. Adv.* **2012**, *30*, 489.

[46] M. H. Wu, C. H. Cheng, C. S. Lai, T. M. Pan, *Sens. Actuators, B* **2009**, *138*, 221.

[47] M. Wu, C. Lee, T. Pan, *Anal. Chim. Acta* **2009**, *651*, 36.

[48] S. K. Jha, A. Topkar, S. F. D'Souza, *J. Biochem. Bioph. Meth.* **2008**, *70*, 1145.

[49] T. Yoshinobu, H. Ecken, A. Poghossian, A. Simonis, H. Iwasaki, H. Lüth, M. J. Schöning, *Electroanalysis* **2001**, *13*, 733.

[50] B. G. Healey, D. R. Walt, *Anal. Chem.* **1995**, *67*, 4471.

[51] S. Lee, M. M. Rahman, K. Sawada, M. Ishida, *Biosens. Bioelectron.* **2009**, *24*, 1877.

[52] S. Beging, M. Leinhos, M. Jablonski, A. Poghossian, M. J. Schöning, *Phys. Status Solidi A* **2015**, *212*, 1353.

[53] Z. H. Ibupoto, S. M. U. Ali, K. Khun, C. O. Chey, O. Nur, M. Willander, *Biosensors* **2011**, *1*, 153.